MHD phenomena in advanced scenarios on ASDEX Upgrade

S. Günter, S. Schade, E. Strumberger, R. Wolf, Q. Yu, ASDEX Upgrade team
Max-Planck-Insitut für Plasmaphysik, EURATOM-association,
D-85748 Garching, Germany

Flat and reversed q-profiles allow the formation of internal transport barriers and thus large pressure gradients since they permit access to second stability with respect to ideal $n \to \infty$ ballooning modes. Reversed magnetic shear gives rise to additional MHD instabilities, unknown in conventional scenarios. Whereas in tokamaks, single tearing modes are expected to be stable, resistive double tearing modes appear if a pair of rational surfaces with the same q-value are close to each other. Large pressure gradients in the weak magnetic shear region drive low-n ballooning modes, so-called infernal modes. Resistive interchange modes can also be driven by a pressure gradient in the negative magnetic shear region. The large pressure gradient at the plasma edge together with the resulting bootstrap current, drive external kink modes unstable, especially in H-mode discharges. Most of these instabilities have been observed in ASDEX Upgrade reversed shear discharges [1].

Double tearing modes (DTMs)

Fig. 1 shows the time development of the q-value on axis and of the minimum q-value for an ASDEX Upgrade reversed shear discharge. When the minimal q-value approaches two, we observe the onset of $(m, n) = (2, 1)$ MHD activity. It starts as fishbone activity, but at about 0.68 s a continuous mode appears. Whereas the fishbone activity does not cause any confinement degradation, as soon as the continuous mode activity sets in, the ion transport barrier breaks down, and the electron temperature decreases as well (Fig. 2). During the mode activity, the current profile is clamped, at least in the vicinity of q_{min}. The end of the (2,1) activity coincides with a sudden drop of q_{min} well below two. According to the stability analyses using the resistive MHD code CASTOR[2], the most unstable mode during this time is a double tearing mode. As shown in Fig. 3, the calculated eigenfunction of this mode agrees well with that measured by electron cyclotron emission (ECE). The eigenfunction has two phase jumps, as expected for a DTM, and a phase shift of 180° between the coupled islands.

To explain the time development of the q-profile, non-linear simulations have been performed in cylindrical geometry using the TM code[3]. It has been shown that the coupled islands are able to flatten the current profile in between the two rational surfaces. This may explain the local clamping of the current profile during the time of the (2,1) DTM activity. About 70 ms after the onset of the (2,1) mode, the mode suddenly disappears, followed by a jump of q_{min} from 2 to about 1.7. This is probably caused by the decoupling of the two tearing modes. Although the minimum q-value does not change during the time of (2,1) mode activity, global current diffusion lowers the q-values everywhere else, resulting in an increasing distance between the two $q = 2$ surfaces. The
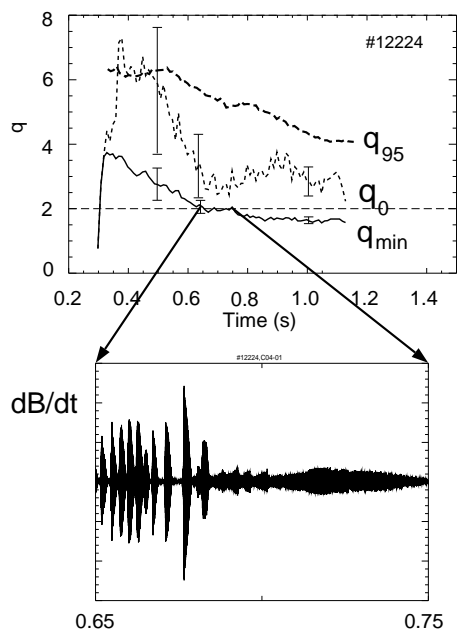
Fig. 1. The time development of the q-value on axis (q_0) and the minimum q-value (q_{min}) are given for ASDEX Upgrade discharge # 12224. During the time in which q_{min} is about 2, the (2,1) activity measured by the Mirnov coils is shown. Between 0.65 and 0.68 s, (2,1) fishbones are observed, whereas afterwards a (2,1) continuous mode appears.
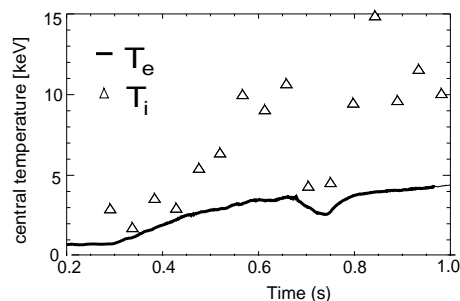

Fig. 2 Central electron (T_e) and ion temperature (T_i) for the same discharge as in Fig. 1, measured by ECE and charge exchange spectroscopy, respectively. The break down of the ion transport barrier, and decreased T_e during the (2,1) continuous mode are seen.
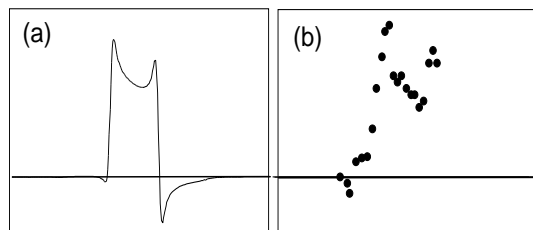

Fig. 3. Eigenfunction of the (2,1) double tearing mode, resulting from the stability analysis compared to that measured by ECE.

growth rate of the DTM, however, strongly depends on the distance between the two rational surfaces. This dependence becomes even stronger if the differential rotation between the two rational surfaces is accounted for. Additional electron heating significantly changes the MHD stability of the discharges considered. With central electron heating applied, the DTM either does not appear if the electron heating is provided before the expected onset of the DTM, or disappeares as soon as the ECRH is switched on. In Fig. 4, the time evolution of the central electron temperature is given for the discharge discussed above in comparison to a discharge with ECRH applied after the onset of the DTM. A few milliseconds after the ECRH has been switched on the electron temperature strongly rises, an electron transport barrier forms in addition to the already existing one for the ion transport [4], accompanied by the disappearance of the DTM. A tentative explanation for this effect could be the increased pressure gradient at the inner $q = 2$ surface, giving rise – in contrast to the dynamics leading to the neoclassical tearing modes in positive shear regions – to a stabilisation of the mode due to the combined effect of bootstrap current reduction in the island and of the negative magnetic shear.
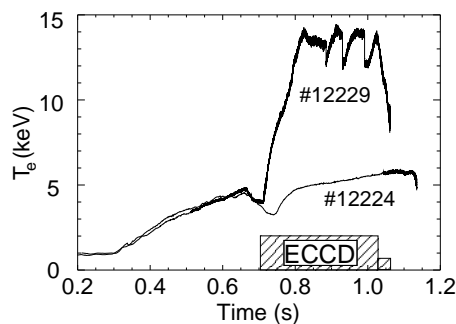

Fig. 4.
Time development of the central electron temperature measured by ECE for a discharge with pure NBI heating (# 12224) and one with combined NBI and ECRH (# 12229).

2. Ideal modes

Sudden drops of the electron temperature during a discharge with combined NBI and EC heating (Fig. 4) indicate the presence of an additional MHD instability. This mode is again a (2,1) mode but grows on a much faster time scale and obviously does not always destroy the internal transport barrier. The evolution of the central electron temperature seems to be similar to that of a sawtoothing discharge with (2,1) instead of (1,1) mode activity limiting the peaking of the temperature profile.
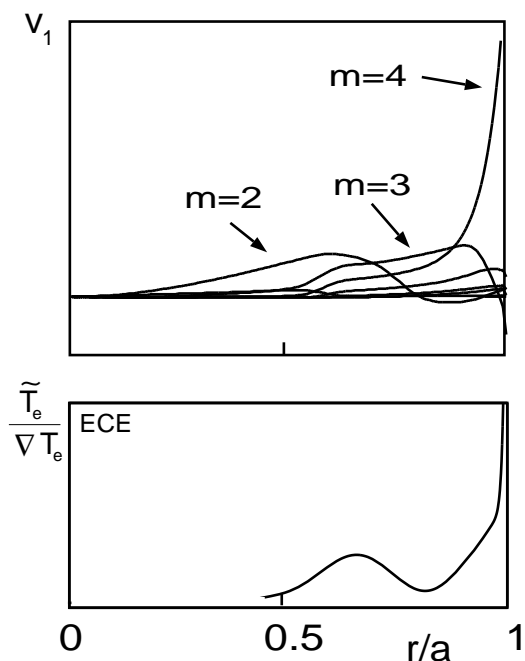

Fig. 5.
Calculated and measured (ECE) eigenfunctions for the mode activity right before the disruption in # 12224. The mode has a large amplitude at the plasma edge, indicating the coupling of the (2,1) infernal mode to the (4,1) external kink.

According to the stability analysis, this mode is an (2,1) infernal mode driven by the pressure gradient in the weak magnetic shear region. Even without additional electron heating, ideal modes often appear in reversed shear discharges, primarily causing disruptions. Characteristic for the q-profiles just before the disruption is a low order rational q-value at the plasma edge, e.g., for the discharge shown in Fig. 1, $q_a \approx 4$. It is obvious that this rational q-value at the plasma edge allows the coupling of the (2,1) infernal mode to an external (4,1) kink mode. As shown in Fig. 5, the eigenfunction resulting from the stability analysis agrees well with the eigenfunction derived from the ECE measurements. The resulting mode is very global, which explains its disruptive character.

3. Optimised q-profiles

The MHD instabilities described above appear due to the occurrence of two low order rational surfaces of the same helicity (DTMs) or due to a large pressure gradient within a weak shear region (infernal modes). An optimised q-profile with respect to the stability of core localised modes has therefore to avoid double rational surfaces. The shear at the low order rational surfaces should be as large as possible, especially in regions with large pressure gradients. Furthermore, in order to avoid the occurrence of neoclassical tearing modes, q_{min} should be larger than 1.5 and the pressure gradient at the $q = 2$ surface should be small.

After an optimisation of the current profile leading to the avoidance of internal modes, the ultimate limit to the normalised plasma pressure is given by external kink modes as l_i is well below 1 for the described q-profiles. These external modes could be stabilised by a wall close to the plasma in combination with a feedback system, which would have to react on the resistive wall time. On ASDEX Upgrade the wall is too far away from the plasma edge to have a significant stabilising effect. Therefore, an additional wall close to the plasma, together with a corresponding feedback system, is under discussion right now. The stabilising effect of an additional ideal wall has been investigated for current profiles expected to be achievable with the current drive capability on ASDEX Upgrade after the movement of one of the NBI injectors into a more tangential orientation. For moderate distance of the wall from the plasma edge ($r_{wall}/r_{plasma} \approx 1.4$) a large stabilising effect has been found allowing for β_N values of about 5 [5].

4. MHD phenomena supporting stationary profiles

Besides their limitation of the achievable normalised plasma pressure in conventional scenarios, MHD instabilities might be helpful in achieving quasi-stationary discharge conditions. As already observed in improved confinement discharges with flat shear, fishbones are able to clamp the current profile locally without any confinement degradation, even in discharges with the minimum q-value (q_{min}) above one[6]. As can be seen in Fig. 1, if there is no $q = 1$ surface inside the plasma, fishbones of different helicities (in this case (2,1) fishbones) can lead to a local clamping of the current profile.

Interestingly, on ASDEX Upgrade it has been observed that the effect of fishbones on the background plasma is significantly different for the two available injection geometries of our NBI system (tangency radii 0.53 m and 0.93 m, respectively, for the more radially and more tangentially oriented beamline groups)[7]. Using only the more radial beam-lines, fishbones have a strong effect on the background plasma, resulting in a limitation of the achievable plasma pressure well below the value expected for the confinement without fishbone activity. Although the fishbone amplitude is even larger if only the more tangential beam lines are used, nearly no effect on confinement is observed. A significant difference between the two beamlines is that the tangential beam sources on ASDEX Upgrade - in contrast to the radial ones - do not directly deposit particles on trapped orbits inside the q = 1 surface.

[1] S. Günter et al., Nucl. Fusion, accepted (2000)
[2] W. Kerner et al. J. Comp. Physics **142**, 271 (1998)
[3] Q. Yu and S. Günter, Nucl. Fusion **39** 487 (1999)
[4] S. Günter et al., Phys. Rev. Lett. **84** 3097 (2000)
[5] S. Saarelma et al. this conference, P 4.065
[6] S. Günter et al., Nucl. Fusion **39**, 1535 (1999)
[7] S. Günter et al., Fusion Engineering and Design, accepted (2000)